

Event-triggered Adaptive Estimated Inverse Neural Network Control of Uncertain Nonlinear Systems With Input Hysteresis Nonlinearity

Jianyong Yao¹, Ning Zhou¹, and Wenxiang Deng¹

¹Nanjing University of Science and Technology School of Mechanical Engineering

September 7, 2023

Abstract

This article investigates an event-triggered adaptive estimated inverse control scheme for a class of uncertain nonlinear systems with hysteresis effects, parametric uncertainties and disturbances. An online estimated inverse hysteresis compensation mechanism is developed, where an adaptive technique is employed to obtain the value of unknown hysteresis parameters. Compared with the common approaches, its biggest advantage lies in that it is not necessary to obtain the hysteresis parameters by means of experiment, which relaxes time-consuming off-line identification work. Moreover, an adaptive radial basis functions neural network (RBFNN) is utilized to approximate the unknown disturbances, whose weight coefficients along with parametric uncertainties are all estimated by the adaptive technique. Besides, the communication cost can be largely saved by introducing the relative threshold event-triggered control (ETC). Through Lyapunov analysis, the proposed controller guarantees the boundedness of all the signals and the convergence of the error signals. The results of numerical simulation illustrate the effectiveness and superiority of the developed controller.

RESEARCH ARTICLE

Event-triggered Adaptive Estimated Inverse Neural Network Control of Uncertain Nonlinear Systems With Input Hysteresis Nonlinearity

Ning Zhou | Jianyong Yao | Wenxiang Deng

¹School of Mechanical Engineering, Nanjing University of Science and Technology, Jiangsu, China

Correspondence

Corresponding author Jianyong Yao, School of Mechanical Engineering, Nanjing University of Science and Technology.

Email: jerryao.buaa@gmail.com

Abstract

This article investigates an event-triggered adaptive estimated inverse control scheme for a class of uncertain nonlinear systems with hysteresis effects, parametric uncertainties and disturbances. An online estimated inverse hysteresis compensation mechanism is developed, where an adaptive technique is employed to obtain the value of unknown hysteresis parameters. Compared with the common approaches, its biggest advantage lies in that it is not necessary to obtain the hysteresis parameters by means of experiment, which relaxes time-consuming off-line identification work. Moreover, an adaptive radial basis functions neural network (RBFNN) is utilized to approximate the unknown disturbances, whose weight coefficients along with parametric uncertainties are all estimated by the adaptive technique. Besides, the communication cost can be largely saved by introducing the relative threshold event-triggered control (ETC). Through Lyapunov analysis, the proposed controller guarantees the boundedness of all the signals and the convergence of the error signals. The results of numerical simulation illustrate the effectiveness and superiority of the developed controller.

KEYWORDS

adaptive law, hysteresis nonlinearities, estimated inverse model, neural network, event-triggered

1 | INTRODUCTION

Hysteresis phenomena widely exist in practical implementations, such as piezoelectric actuators^{1,2} and proportional solenoids^{3,4}. It is quite a challenge to control such systems with hysteresis nonlinearities, as the hysteresis effect is typically unknown, non-differentiable and multi-valued in practice. The system will tend to exhibit undesirable performance such as oscillation or even instability^{5,6,7}, if the hysteresis effects are not considered and compensated properly. The actual system still includes parametric uncertainties and disturbances besides hysteresis effects, which makes the controller design quite challenging.

In the past decades, numerous advanced controllers have been proposed to handle both parametric uncertainties and disturbances together. For instance, adaptive robust control (ARC) method developed in⁸ where the adaptive term compensates the parametric uncertainties and the robust term suppresses the unknown disturbances, has been widely applied to plenty of engineering applications, such as active suspension systems⁹, linear motors¹⁰, underwater hydraulic manipulator¹¹, etc. Due to the simple structure and strong robustness, the sliding mode control (SMC) scheme has been widely employed to mitigate unknown disturbances. The adaptive sliding mode control (ASMC) obtained¹² by integrating SMC with adaptive control (AC), can also suppress parametric uncertainties and disturbances both existing in control system. Additionally, as a typical variant of ASMC, adaptive terminal sliding mode control (ATSMC) gains increasing popularity among such systems that still demand finite-time stability. Moreover, considering the excellent ability to estimate unknown disturbances, various disturbance observers have attracted much attention, such as extended state observer, disturbance observer^{13,14}, sliding mode observer¹⁵, etc. However, such observer-based control scheme takes both parametric uncertainties and disturbances as generalized disturbances ignoring the characteristic of parametric uncertainties. In¹⁶, the active disturbance rejection adaptive control is formulated by integrating

the adaptive control and the disturbance observer, where parametric uncertainties are estimated by the adaptive technique and unknown disturbances are approximated and compensated by the observer. In view of the universal approximation property of fuzzy logic system and neural network, the controllers including either of them have been well studied recently. In¹⁷, the fuzzy logic systems is developed to approximate the unknown disturbances. In¹⁸, the neural network integrated with the adaptive control is formulated to control a DC motor with parametric uncertainties, external disturbances along with unmeasured system states.

However, the above-mentioned controllers cannot guarantee the uniformity of performance if they are directly used in a general actual system subjected to hysteresis nonlinearities, parametric uncertainties and disturbances at the same time. As hysteresis nonlinearities are totally different from parametric uncertainties and disturbances, the controllers may malfunction without taking hysteresis effects into account. Therefore, it is necessary to design a comprehensive controller with special hysteresis compensation mechanism. To this end, finding proper hysteresis models is primarily significant to compensate them, and there are plenty of models that have been developed such as Preisach model¹⁹, Prandtl-Ishlinskii hysteresis operator²⁰, Bouc-Wen differential model²¹. Based on these models, promising progresses have been made on the control schemes which can compensate the hysteresis nonlinearities to some extent. Generally speaking, the existing control methods can be divided into two categories. The first one is to directly divide the hysteresis model into linear and nonlinear part without constructing its inverse model. Since it is impossible to acquire the accurate hysteresis model, the linear part is always represented by the product of an unknown coefficient and the control signal, the nonlinear part is a unknown term constituted by hysteresis operators. It is typical that the linear part is treated as a parametric uncertainty and the nonlinear part is simply dealt with as disturbance in many literature^{6,7,22,23,24,25,26,27}. These controllers fuse the nonlinear part derived from the hysteresis model with the other system disturbances directly and compensate them together, ignoring the nature of hysteresis effects. Different from such approach, the control schemes proposed in^{6,7,25,26,27} devise adaptive laws for the hysteresis operators of the nonlinear part and compensate it via the feed-forward model-based compensation term. Nevertheless, these methods of compensating hysteresis do not figure out the nature of hysteresis effects completely. The inverse compensation strategy is an ideal way where the hysteresis inverse model is formulated and cascaded into the controller design. Since the precise inverse hysteresis model is hard to obtain, it is necessary to construct the estimated hysteresis inverse model.^{28,29,30,31,32} Numerous estimated inverse control schemes^{29,30,33,34} have been developed where the hysteresis model is replaced with its estimated inverse one based on the compensation error between them. However, the estimated hysteresis inverse compensation have to identify th unknown hysteresis parameters through experimental results, which incurs extra cost in implementing those controllers. In addition, it is assumed that the controller compensating hysteresis effects may require more calculation resources²³. Thus, to reduce the communication burden and maintain the system performance, the event-triggered control(ETC) has attracted increasing interest^{35,36,37}. So far, for general nonlinear systems subjected to hysteresis nonlinearities, parametric uncertainties and disturbances, how to develop an applicable controller with estimated hysteresis inverse compensation online and event-triggered control has not been adequately investigated.

Motivated by the aforementioned discussion, an event-triggered adaptive estimated inverse neural network controller is proposed for a class of general uncertain nonlinear systems. The contributions are listed as follows.

- To our best knowledge, it is the first time to investigate the tracking control problem of general nonlinear systems subjected to parametric uncertainties, disturbances along with unknown hysteresis effect characterized by Prandtl-Ishlinskii model.
- The direct hysteresis compensation methods do not fully consider the nature of hysteresis effect and the existing inverse hysteresis compensation methods require tedious experimental identification work. Different from those two types of methods, an online estimated inverse compensation scheme is proposed whose unknown hysteresis parameters are updated online.
- To decrease communication burden brought from the hysteresis compensation controller based on time-triggered mechanism, a relative-threshold event-triggered control mechanism is incorporated into the proposed controller.

The rest parts of this paper are organized as follows. The problem formulation and preliminaries are presented in Section II. Section III describes the detailed controller design process and gives the stability analysis. To demonstrate the feasibility of the proposed controller, numerical simulation results are presented in Section IV. Finally, Section V shows some conclusions of this article.

2 | PROBLEM FORMULATION AND PRELIMINARIES

2.1 | System Description

Consider the following uncertain nonlinear system

$$\begin{cases} \dot{x}_i = x_{i+1} + \boldsymbol{\theta}^T \phi_i(\bar{x}_i) + \Delta_i(\bar{x}_i, t) & i = 1, 2, \dots, n-1 \\ \dot{x}_n = u + \boldsymbol{\theta}^T \phi_n(\mathbf{x}) + \Delta_n(\mathbf{x}, t) \\ y = x_1, u = H[v](t) \end{cases} \quad (1)$$

where $\bar{x}_i = [x_1, \dots, x_i]^T \in \mathfrak{R}^i$ and $\mathbf{x} = [x_1, \dots, x_n]^T \in \mathfrak{R}^n$ are the state vectors, and $y \in \mathfrak{R}$ represents the system output signal. $u \in \mathfrak{R}$ is control input subjected to unknown hysteresis nonlinearities. The hysteresis model $H[v](t)$ is represented by Prandtle-Ishlinskii model and its specific expression will be given subsequently. $\boldsymbol{\theta} = [\theta_1, \theta_2, \dots, \theta_p]^T \in \mathfrak{R}^p$ is the vector of unknown parameters, $\phi_1, \dots, \phi_n \in \mathfrak{R}^p$ are known smooth nonlinear functions, $\Delta_i(\bar{x}_i, t) : \mathfrak{R}^i \rightarrow \mathfrak{R} (i = 1, 2, \dots, n)$ are disturbances.

Remark 1. The considered nonlinear system model can describe plenty of actual mechanical equipment such as the piezoelectric positioning stages studied in many literature^{2,30,34}. Their system parameters, such as the fixed gain of the voltage power amplifier, the equivalent internal resistance, may be unknown, which can be treated as parametric uncertainties in (1). Additionally, the stage may be subjected to external disturbance such as nonlinear friction and unmodeled dynamics, which can be seen as disturbances in (1). Furthermore, the inherent hysteresis nonlinearities are unavoidably in view of its structure and principle. Thus, the nonlinear system in (1) describing the complex characteristic of such systems should be given more attention.

The subjective of this paper is to construct an event-triggered adaptive estimated inverse neural network control scheme for the general nonlinear systems described in (1) subjected to parametric uncertainties, unknown nonlinear functions and unknown hysteresis effects, such that the system output signal y can track a given reference trajectory x_{1d} precisely and all the system signals are bounded.

2.2 | Radial Basis Function Neural Networks

To deal with the unknown nonlinear functions, the radial basis function neural network is employed. It has been pointed out in many literature^{38,39,40} that RBFNN shows excellent universe approximation property which can be used to estimate any continuous functions with arbitrary accuracy, it follow that

$$f(\mathbf{s}) = \boldsymbol{\nu}^{*T} \boldsymbol{\zeta}(\mathbf{s}) + \delta \quad (2)$$

where $\mathbf{s} \in \mathfrak{R}^l$ is input vector and $\boldsymbol{\nu}^* = [\nu_1^*, \dots, \nu_m^*]^T \in \mathfrak{R}^m$ is the optimal weight vector of RBFNN and $\boldsymbol{\zeta} = [\zeta_1(\mathbf{s}), \dots, \zeta_m(\mathbf{s})]^T \in \mathfrak{R}^m$ is the activation function vector. δ is approximation error from neural network. The following Gaussian function is utilized to denote $\zeta_i(\mathbf{s})$:

$$\zeta_i(\mathbf{s}) = \exp \left[-\frac{(\mathbf{s} - \mathbf{c}_i)^T (\mathbf{s} - \mathbf{c}_i)}{d_i^2} \right] \quad i = 1, \dots, m \quad (3)$$

where $\mathbf{c}_i = [c_{i1}, \dots, c_{il}]^T \in \mathfrak{R}^l$ is center of the receptive field and d_i is the width of Gaussian functions.

The ideal weight vector of RBFNN is obtained when the following equation holds

$$\boldsymbol{\nu}^* := \arg \min_{\boldsymbol{\nu} \in \mathfrak{R}^m} \{ \sup_{\mathbf{s} \in \mathfrak{R}^l} |f(\mathbf{s}) - \boldsymbol{\nu}^T \boldsymbol{\zeta}(\mathbf{s})| \} \quad (4)$$

Remark 2. Since it is hard to obtain the ideal weights, we usually employ $\boldsymbol{\nu}^T \boldsymbol{\zeta}(\mathbf{s})$ to estimate the unknown nonlinear functions. $\boldsymbol{\nu}$ is the estimation of the variable $\boldsymbol{\nu}^*$ and will be obtained based on the adaptive technique online. The deviation $\tilde{\boldsymbol{\nu}} = \boldsymbol{\nu} - \boldsymbol{\nu}^*$ is proven to be bounded in the following stability analysis.

2.3 | PI Model and its inverse model

Firstly, we give the expression of PI hysteresis model based on play operator and construct its corresponding estimated inverse model. Subsequently, the parameterized error between hysteresis model and its estimated inverse is developed.

The definition of play operator⁶ is given by

$$\begin{aligned} F_r[v](0) &= f_r(v(0), 0) \\ F_r[v](t) &= f_r(v(t), F_r[v](t_i)) \\ &\text{for } t_i < t < t_{i+1}; 0 \leq i \leq N-1 \end{aligned} \quad (5)$$

where $f_r(v, u) = \max\{v-r, \min\{v+r, u\}\}$, $0 = t_0 < t_1 < \dots < t_N = t_E$ is a partition of $[0, t_E]$ guaranteeing that the signal function $v(t)$ is monotone on each of the sub-intervals $(t_i, t_{i+1}]$.

According to the play operator $F_r[v](t)$, PI hysteresis model $H[v](t)$ can be defined as:

$$u(t) = H[v](t) = p_{0s}v(t) - \int_0^R p(r)F_r[v](t)dr \quad (6)$$

where p_{0s} is a positive constant and $p(r)$ denotes density function holding with $p(r) \geq 0$. The upper bound of integration is set as R instead of ∞ as $p(r)$ will vanish to zero for large values of r .

To facilitate the control design and implementation, the corresponding hysteresis discrete expression $H_L[v](t)$ is applied.

$$\begin{aligned} u(t) &= H[v](t) = H_L[v](t) + \epsilon(t) \\ &= p_{0s}v(t) - \sum_{i=1}^m p(r_i)F_{r_i}[v](t)\Delta r_i + \epsilon(t) \end{aligned} \quad (7)$$

where m denotes the number of the discrete intervals and Δr_i is the length of the interval, $\epsilon(t)$ denotes the approximation error between continuous model and discrete model.

Due to the length of the discrete intervals Δr_i is often set as a fixed constant, we can define a new variable $\theta_i = p_i\Delta r_i$ to simplify the expression

$$H_L[v](t) = p_{0s}v(t) - \sum_{i=1}^m \theta_i F_{r_i}[v](t) \quad (8)$$

Remark 3. Noting that the p_{0s} and θ_i are unknown since they are related to the density function that is hard to obtain in practical application. According to the definition of play operator in (5), $F_r[v](t)$ is a certain function where the hysteresis threshold r is also set artificially, and the output signal and the input signal of the play operator can also be obtained.

Since it is quite difficult to acquire the accurate density function, the estimated hysteresis model is introduced

$$u_d(t) = \hat{p}_{0s}v(t) - \sum_{i=1}^m \hat{\theta}_i F_{r_i}[v](t) \quad (9)$$

where \hat{p}_{0s} and $\hat{\theta}_i$ are the estimation of p_{0s} and θ_i , respectively, u_d is the desired control signal.

According to the estimated hysteresis model (9), the expression of estimated hysteresis inverse model can be defined as

$$v(t) = H_L^{-1}[u_d](t) = \hat{p}'_{0s}u_d(t) - \sum_{i=1}^m \hat{\theta}'_i F_{r_i}[u_d](t) \quad (10)$$

where

$$\begin{aligned}
 p'_{0s} &= \frac{1}{\hat{p}_{0s}} \\
 \hat{\theta}'_i &= -\frac{\hat{\theta}_i}{(p'_{0s} + \sum_{j=1}^i \hat{\theta}_j)(\hat{p}_{0s} + \sum_{j=1}^{i-1} \hat{\theta}_j)} \\
 r'_i &= \hat{p}_{0s} r_i + \sum_{j=1}^{i-1} \hat{\theta}_j (r_i - r_j) \\
 \hat{p}'_{0s} &= \sum_{i=1}^m \hat{\theta}'_i
 \end{aligned} \tag{11}$$

Remark 4. By observing the inverse model (10) and (11), it is can be found that the variable p'_{0s} and $\hat{\theta}'_i$ are defined by p_{0s} and $\hat{\theta}_i$ essentially. Thus, we just employ the adaptive law to estimate p_{0s} and $\hat{\theta}_i$ on which p'_{0s} and $\hat{\theta}'_i$ can be calculated based.

The control scheme of estimated hysteresis inverse compensation is depicted in Fig. 1. It should be mentioned that there are four control signals in the whole process, namely the desired control signal $u_d(t)$, the intermediate control signal $v(t)$, the event-triggered output control signal $\omega(t)$ and the actual control signal $u(t)$. From the blue line and block, we can know that the core of estimated inverse compensation lies in that the signal experiencing estimated inverse hysteresis model and hysteresis model successively will exhibit almost free-hysteresis performance, which results in an excellent hysteresis compensation effect.

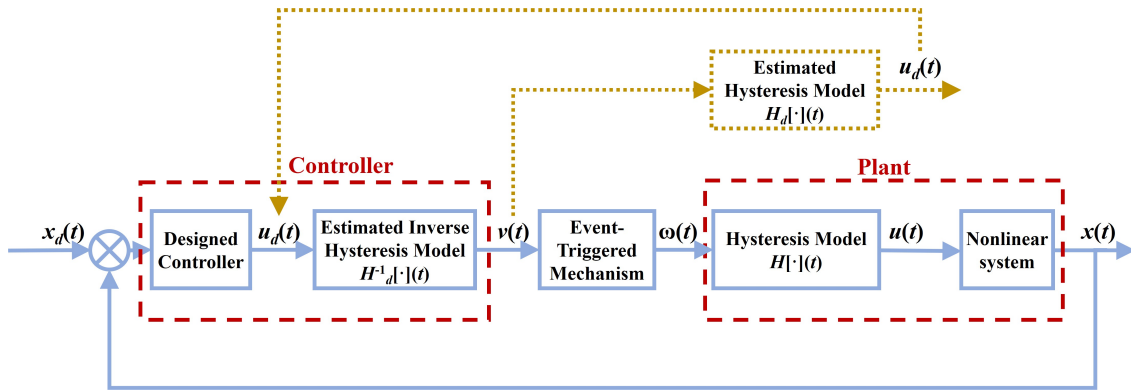


FIGURE 1 Estimated inverse compensation scheme of hysteresis.

Remark 5. Actually, the controller includes two part: the designed controller and the estimated inverse hysteresis model. The desired control signal $u_d(t)$ experiences the estimated inverse hysteresis model generating the intermediate control signal $v(t)$. The adaptive technique is utilized to obtain the unknown parameters of inverse model, which relaxes the requirements on parameter identification. To save the communication resource, the relative threshold event-triggered law is introduced. It should be mentioned that the event-triggered output control signal $\omega(t)$ is the eventual designed control signal and the actual control signal $u(t)$ is not the result of the control design. The hysteresis model is fused with the nonlinear system as the plant to be controlled. It is worth noting that the hysteresis model is completely unknown, and the control signal $u(t)$ after it is the actual control signal acting on the actuator system.

Remark 6. As for the yellow line and block in Fig. 1, this part does not participate in the practical control process directly. If we observe the estimated hysteresis inverse model $H_d^{-1}[\cdot](t)$ block and the estimated hysteresis model $H_d[\cdot](t)$, it is easy for us to understand the inverse compensation nature. Since the actual hysteresis model is unknown, the inverse model is constructed based on the estimated model.

From (7) and (9), the deviation is given as

$$u(t) - u_d(t) = \tilde{p}_{0s}v(t) - \sum_{i=1}^m \tilde{\theta}_i F_{r_i}[v](t) + \epsilon(t) \quad (12)$$

where $\tilde{p}_{0s} = p_{0s} - \hat{p}_{0s}$ and $\tilde{\theta}_i = \theta_i - \hat{\theta}_i$. Rearrange (12) into a parameterized form, which is more conducive to controller design.

$$u(t) - u_d(t) = \tilde{\boldsymbol{\theta}}^T \mathbf{F} + \epsilon(t) \quad (13)$$

where $\tilde{\boldsymbol{\theta}} = [\tilde{p}_{0s}, -\tilde{\theta}_1, -\tilde{\theta}_2, \dots, -\tilde{\theta}_m]^T$ and $\tilde{\boldsymbol{\theta}} = \boldsymbol{\theta} - \hat{\boldsymbol{\theta}}$, $\boldsymbol{\theta} = [p_{0s}, -\theta_1, -\theta_2, \dots, -\theta_m]^T$, $\hat{\boldsymbol{\theta}} = [\hat{p}_{0s}, -\hat{\theta}_1, -\hat{\theta}_2, \dots, -\hat{\theta}_m]^T$, $\mathbf{F} = [v(t), F_{r_1}[v](t), F_{r_2}[v](t), \dots, F_{r_m}[v](t)]^T$.

Before carrying out the controller design, the following assumptions and inequalities are necessary for the design of the controller.

Assumption 1. The desired trajectory $x_{1d}(t)$ and its $(n + 1)$ th order derivatives are certain and bounded.

Assumption 2. The approximation error from neural network δ and error from discrete model $\epsilon(t)$ are both bounded, satisfying $|\delta| \leq \iota$ and $\epsilon(t) < \bar{\epsilon}$ where ι and $\bar{\epsilon}$ are positive constants.

Assumption 3. System disturbances $\Delta_i(\bar{x}_i, t)$ are continuous and smooth.

According to Young's inequality, the upper boundedness of δ , the upper boundedness of $\epsilon(t)$ and the definition of $\tilde{\boldsymbol{\nu}}$, the following inequality holds:

$$z_i \delta_i \leq \frac{1}{2} z_i^2 + \frac{1}{2} \iota_i^2 \quad (14)$$

$$z_n \epsilon(t) \leq \frac{1}{2} z_n^2 + \frac{1}{2} \bar{\epsilon}^2 \quad (15)$$

$$\tilde{\boldsymbol{\nu}}_i^T \boldsymbol{\nu}_i \leq -\frac{1}{2} \tilde{\boldsymbol{\nu}}_i^T \tilde{\boldsymbol{\nu}}_i + \frac{1}{2} \boldsymbol{\nu}_i^{*T} \boldsymbol{\nu}_i^* \quad (16)$$

3 | EVENT-TRIGGERED ADAPTIVE INVERSE CONTROL DESIGN AND STABILITY ANALYSIS

3.1 | Controller design

First, the following the error variables are defined as:

$$\begin{cases} z_1 = x_1 - x_{1d} \\ z_i = x_i - \alpha_{i-1} - x_{1d}^{(i-1)} \quad i = 2, 3, \dots, n \end{cases} \quad (17)$$

where α_{i-1} is the virtual control law and z_i is the error variable.

Step 1: By (1) and (17), the derivative of z_1 can be given as

$$\dot{z}_1 = z_2 + \alpha_1 + \boldsymbol{\theta}^T \boldsymbol{\phi}_1(x_1) + \Delta_1(x_1, t) \quad (18)$$

The RBFNN is utilized to approximate the nonlinear function $\Delta_1(x_1, t)$, that is

$$\dot{z}_1 = z_2 + \alpha_1 + \boldsymbol{\theta}^T \boldsymbol{\phi}_1(x_1) + \boldsymbol{\nu}_1^{*T} \boldsymbol{\zeta}_1(x_1) + \delta_1 \quad (19)$$

Therefore, the virtual control law α_1 , the tuning function $\boldsymbol{\tau}_1$ and the adaptive law $\dot{\boldsymbol{\nu}}_1$ for weights of RBFNN are given as

$$\begin{cases} \alpha_1 = -k_1 z_1 - \hat{\boldsymbol{\theta}}^T \boldsymbol{\phi}_1(x_1) - \boldsymbol{\nu}_1^T \boldsymbol{\zeta}_1(x_1) \\ \boldsymbol{\tau}_1 = \boldsymbol{\phi}_1(x_1) z_1 \\ \dot{\boldsymbol{\nu}}_1 = \mathbf{P}_1 \boldsymbol{\zeta}_1(x_1) z_1 - b_1 \mathbf{P}_1 \boldsymbol{\nu}_1 \end{cases} \quad (20)$$

where $k_1 > 0, b_1 > 0$ are positive constants, $\hat{\theta}$ is the estimator of θ and \mathbf{P}_1 is a positive definite matrix.

Substituting (20) into (19), results in

$$\dot{z}_1 = z_2 - k_1 z_1 + \tilde{\theta}^T \phi_1(x_1) + \tilde{\nu}_1^T \zeta_1(x_1) + \delta_1 \quad (21)$$

Choose the Lyapunov function candidate V_1 as

$$V_1 = \frac{1}{2} z_1^2 + \frac{1}{2} \tilde{\theta}^T \Gamma_\theta^{-1} \tilde{\theta} + \frac{1}{2} \tilde{\nu}_1^T \mathbf{P}_1^{-1} \tilde{\nu}_1 \quad (22)$$

where Γ_θ is a positive definite matrix.

Invoking (14), (16) and (21), the derivative of V_1 yields

$$\begin{aligned} \dot{V}_1 &= z_1(z_2 - k_1 z_1 + \tilde{\theta}^T \phi_1(x_1) + \tilde{\nu}_1^T \zeta_1(x_1) + \delta_1) - \tilde{\theta}^T \Gamma_\theta^{-1} \dot{\tilde{\theta}} - \tilde{\nu}_1^T \mathbf{P}_1^{-1} \dot{\tilde{\nu}}_1 \\ &\leq z_1 z_2 - k_1 z_1^2 + \tilde{\nu}_1^T (z_1 \zeta_1(x_1) - \mathbf{P}_1^{-1} \dot{\tilde{\nu}}_1) + \tilde{\theta}^T (\tau_1 - \Gamma_\theta^{-1} \dot{\tilde{\theta}}) + z_1 \delta_1 \\ &\leq -\left(k_1 - \frac{1}{2}\right) z_1^2 + z_1 z_2 - \frac{b_1}{2} \tilde{\nu}_1^T \tilde{\nu}_1 + \tilde{\theta}^T (\tau_1 - \Gamma_\theta^{-1} \dot{\tilde{\theta}}) + \eta_1 \end{aligned} \quad (23)$$

where $\eta_1 = \frac{1}{2} \nu_1^{*2} + \frac{b_1}{2} \nu_1^{*T} \nu_1^*$

Step 2: Differentiating z_2 yields

$$\dot{z}_2 = z_3 + \alpha_2 + \theta^T \phi_2(\bar{x}_2) + \Delta_2(\bar{x}_2, t) - \frac{\partial \alpha_1}{\partial x_1} (x_2 + \theta^T \phi_1(\bar{x}_1) + \Delta_1(\bar{x}_1, t)) - \frac{\partial \alpha_1}{\partial x_{1d}} \dot{x}_{1d} - \frac{\partial \alpha_1}{\partial \nu_1^T} \dot{\nu}_1 - \frac{\partial \alpha_1}{\partial \hat{\theta}^T} \dot{\hat{\theta}} \quad (24)$$

An RBFNN $\nu_2^{*T} \zeta_2(\bar{x}_2) + \delta_2$ is employed to estimate $\Delta_2(\bar{x}_2, t) - \frac{\partial \alpha_1}{\partial x_1} \Delta_1(x_1, t)$, that is

$$\Delta_2(\bar{x}_2, t) - \frac{\partial \alpha_1}{\partial x_1} \Delta_1(x_1, t) = \nu_2^{*T} \zeta_2(\bar{x}_2) + \delta_2 \quad (25)$$

Then the virtual control law α_2 , the tuning function τ_2 and the adaptive law $\dot{\nu}_2$ are proposed as

$$\begin{cases} \alpha_2 = -k_2 z_2 - z_1 + \frac{\partial \alpha_1}{\partial x_1} x_2 - \nu_2^T \zeta_2(\bar{x}_2) - \hat{\theta}^T (\phi_2(\bar{x}_2) - \frac{\partial \alpha_1}{\partial x_1} \phi_1(x_1)) + \frac{\partial \alpha_1}{\partial x_{1d}} \dot{x}_{1d} + \frac{\partial \alpha_1}{\partial \hat{\theta}^T} \Gamma_\theta (\tau_2 - \sigma \hat{\theta}) + \frac{\partial \alpha_1}{\partial \nu_1^T} \dot{\nu}_1 \\ \tau_2 = \tau_1 + (\phi_2(\bar{x}_2) - \frac{\partial \alpha_1}{\partial x_1} \phi_1(x_1)) z_2 \\ \dot{\nu}_2 = \mathbf{P}_2 \zeta_2(\bar{x}_2) z_2 - b_2 \mathbf{P}_2 \nu_2 \end{cases} \quad (26)$$

where $k_2 > 0, b_2 > 0$ are positive constants to be designed, \mathbf{P}_2 is a positive definite matrix.

Substituting (25) and (26) into (24), we have

$$\dot{z}_2 = z_3 - k_2 z_2 - z_1 + \tilde{\nu}_2^T \zeta_2(\bar{x}_2) + \tilde{\theta}^T (\phi_2(\bar{x}_2) - \frac{\partial \alpha_1}{\partial x_1} \phi_1(x_1)) + \frac{\partial \alpha_1}{\partial \hat{\theta}^T} \Gamma_\theta (\tau_2 - \sigma \hat{\theta} - \Gamma_\theta^{-1} \dot{\tilde{\theta}}) + \delta_2 \quad (27)$$

Choose the Lyapunov function V_2 as

$$V_2 = V_1 + \frac{1}{2} z_2^2 + \frac{1}{2} \tilde{\nu}_2^T \mathbf{P}_2^{-1} \tilde{\nu}_2 \quad (28)$$

where $\tilde{\nu}_2 = \nu_2^* - \nu_2$.

Considering (14), (16), (23) and (27), the derivative of V_2 satisfies the following inequality

$$\begin{aligned} \dot{V}_2 &= z_1 z_2 - \left(k_1 - \frac{1}{2}\right) z_1^2 + \tilde{\theta}^T (\tau_1 - \Gamma_\theta^{-1} \dot{\tilde{\theta}}) - \frac{b_1}{2} \tilde{\nu}_1^T \tilde{\nu}_1 + z_2 \left(z_3 - k_2 z_2 - z_1 + \tilde{\nu}_2^T \zeta_2(\bar{x}_2) + \delta_2 \right. \\ &\quad \left. + \tilde{\theta}^T (\phi_2(\bar{x}_2) - \frac{\partial \alpha_1}{\partial x_1} \phi_1(x_1)) + \frac{\partial \alpha_1}{\partial \hat{\theta}^T} \Gamma_\theta (\tau_2 - \sigma \hat{\theta}) - \frac{\partial \alpha_1}{\partial \hat{\theta}^T} \dot{\tilde{\theta}} \right) - \tilde{\nu}_2^T \mathbf{P}_2^{-1} \dot{\tilde{\nu}}_2 + \eta_1 \\ &\leq -\left(k_1 - \frac{1}{2}\right) z_1^2 - \left(k_2 - \frac{1}{2}\right) z_2^2 + z_2 z_3 - \frac{b_1}{2} \tilde{\nu}_1^T \tilde{\nu}_1 - \frac{b_2}{2} \tilde{\nu}_2^T \tilde{\nu}_2 + \tilde{\theta}^T (\tau_2 - \Gamma_\theta^{-1} \dot{\tilde{\theta}}) + z_2 \frac{\partial \alpha_1}{\partial \hat{\theta}^T} \Gamma_\theta (\tau_2 - \sigma \hat{\theta} - \Gamma_\theta^{-1} \dot{\tilde{\theta}}) + \eta_2 \end{aligned} \quad (29)$$

where $\eta_2 = \sum_{j=1}^2 \left(\frac{b_j}{2} \nu_j^{*T} \nu_j^* + \frac{1}{2} l_j^2 \right)$

Step i: ($3 \leq i \leq n-1$) The derivative of z_i is defined as

$$\dot{z}_i = z_{i+1} + \alpha_i + \boldsymbol{\theta}^T \boldsymbol{\phi}_i(\bar{\mathbf{x}}_i) + \Delta_i(\bar{\mathbf{x}}_i, t) - \sum_{j=1}^{i-1} \frac{\partial \alpha_{i-1}}{\partial x_j} (x_{j+1} + \boldsymbol{\theta}^T \boldsymbol{\phi}_j(\bar{\mathbf{x}}_j) + \Delta_j(\bar{\mathbf{x}}_j, t)) - \sum_{j=1}^{i-1} \frac{\partial \alpha_{i-1}}{\partial x_{1d}^{(j-1)}} x_{1d}^{(j)} - \sum_{j=1}^{i-1} \frac{\partial \alpha_{j-1}}{\partial \hat{\boldsymbol{\nu}}_j^T} \dot{\hat{\boldsymbol{\nu}}}_j - \frac{\partial \alpha_{i-1}}{\partial \hat{\boldsymbol{\theta}}^T} \dot{\hat{\boldsymbol{\theta}}} \quad (30)$$

An RBFNN $\boldsymbol{\nu}_i^{*T} \boldsymbol{\zeta}_i(\bar{\mathbf{x}}_i) + \delta_i$ is utilized to approximate $\Delta_i(\bar{\mathbf{x}}_i, t) - \sum_{j=1}^{i-1} \frac{\partial \alpha_{i-1}}{\partial x_j} \Delta_j(\bar{\mathbf{x}}_j, t)$, that is

$$\Delta_i(\bar{\mathbf{x}}_i, t) - \sum_{j=1}^{i-1} \frac{\partial \alpha_{i-1}}{\partial x_j} \Delta_j(\bar{\mathbf{x}}_j, t) = \boldsymbol{\nu}_i^{*T} \boldsymbol{\zeta}_i(\bar{\mathbf{x}}_i) + \delta_i \quad (31)$$

Now, virtual control law α_i , the tuning function τ_i and the adaptive law $\dot{\boldsymbol{\nu}}_i$ are developed as

$$\begin{cases} \alpha_i = -k_i z_i - z_{i-1} + \sum_{j=1}^{i-1} \frac{\partial \alpha_{i-1}}{\partial x_j} x_{j+1} - \boldsymbol{\nu}_i^T \boldsymbol{\zeta}_i(\bar{\mathbf{x}}_i) - \hat{\boldsymbol{\theta}}^T (\boldsymbol{\phi}_i(\bar{\mathbf{x}}_i) - \sum_{j=1}^{i-1} \frac{\partial \alpha_{i-1}}{\partial x_j} \boldsymbol{\phi}_j(\bar{\mathbf{x}}_j)) + \sum_{j=1}^{i-1} \frac{\partial \alpha_{i-1}}{\partial x_{1d}^{(j-1)}} x_{1d}^{(j)} \\ \quad + \frac{\partial \alpha_{i-1}}{\partial \hat{\boldsymbol{\theta}}^T} \boldsymbol{\Gamma}_\theta (\boldsymbol{\tau}_i - \sigma \hat{\boldsymbol{\theta}}) + \sum_{j=1}^{i-1} \frac{\partial \alpha_{j-1}}{\partial \hat{\boldsymbol{\nu}}_j^T} \dot{\hat{\boldsymbol{\nu}}}_j \\ \tau_i = \tau_{i-1} + (\boldsymbol{\phi}_i(\bar{\mathbf{x}}_i) - \sum_{j=1}^{i-1} \frac{\partial \alpha_{i-1}}{\partial x_j} \boldsymbol{\phi}_j(\bar{\mathbf{x}}_j)) z_i \\ \dot{\hat{\boldsymbol{\nu}}}_i = \mathbf{P}_i \boldsymbol{\zeta}_i(\bar{\mathbf{x}}_i) z_i - b_i \mathbf{P}_i \boldsymbol{\nu}_i \end{cases} \quad (32)$$

where $k_i > 0$, $b_i > 0$ are positive constants to be designed, \mathbf{P}_i is a positive definite matrix.

Substituting (31) and (32) into (30), one has

$$\dot{z}_i = z_{i+1} - k_i z_i - z_{i-1} + \tilde{\boldsymbol{\nu}}_i^T \boldsymbol{\zeta}_i(\bar{\mathbf{x}}_i) + \delta_i + \tilde{\boldsymbol{\theta}}^T (\boldsymbol{\phi}_i(\bar{\mathbf{x}}_i) - \sum_{j=1}^{i-1} \frac{\partial \alpha_{i-1}}{\partial x_j} \boldsymbol{\phi}_j(\bar{\mathbf{x}}_j)) + \frac{\partial \alpha_{i-1}}{\partial \hat{\boldsymbol{\theta}}^T} \boldsymbol{\Gamma}_\theta (\boldsymbol{\tau}_i - \sigma \hat{\boldsymbol{\theta}} - \boldsymbol{\Gamma}_\theta^{-1} \dot{\hat{\boldsymbol{\theta}}}) \quad (33)$$

Consider the following Lyapunov function candidate V_i as

$$V_i = V_{i-1} + \frac{1}{2} z_i^2 + \frac{1}{2} \tilde{\boldsymbol{\nu}}_i^T \mathbf{P}_i^{-1} \tilde{\boldsymbol{\nu}}_i \quad (34)$$

Invoking (14), (16) and (33), the derivative of V_i yields

$$\begin{aligned} \dot{V}_i &= \dot{V}_{i-1} + z_i \dot{z}_i - \tilde{\boldsymbol{\nu}}_i^T \mathbf{P}_i^{-1} \dot{\tilde{\boldsymbol{\nu}}}_i \\ &\leq - \sum_{j=1}^{i-1} (k_j - \frac{1}{2}) z_j^2 + z_{i-1} z_i - \sum_{j=1}^{i-1} \frac{b_j}{2} \tilde{\boldsymbol{\nu}}_j^T \tilde{\boldsymbol{\nu}}_j + \tilde{\boldsymbol{\theta}}^T (\boldsymbol{\tau}_{i-1} - \boldsymbol{\Gamma}_\theta^{-1} \dot{\hat{\boldsymbol{\theta}}}) + \eta_{i-1} - \sum_{j=2}^{i-1} z_j \frac{\partial \alpha_{j-1}}{\partial \hat{\boldsymbol{\theta}}^T} \boldsymbol{\Gamma}_\theta (\boldsymbol{\tau}_{i-1} - \sigma \hat{\boldsymbol{\theta}} - \boldsymbol{\Gamma}_\theta^{-1} \dot{\hat{\boldsymbol{\theta}}}) \end{aligned} \quad (35)$$

$$+ z_i \left(z_{i+1} - k_i z_i - z_{i-1} + \tilde{\boldsymbol{\nu}}_i^T \boldsymbol{\zeta}_i(\bar{\mathbf{x}}_i) + \delta_i + \tilde{\boldsymbol{\theta}}^T (\boldsymbol{\phi}_i(\bar{\mathbf{x}}_i) - \sum_{j=1}^{i-1} \frac{\partial \alpha_{i-1}}{\partial x_j} \boldsymbol{\phi}_j(\bar{\mathbf{x}}_j)) + \frac{\partial \alpha_{i-1}}{\partial \hat{\boldsymbol{\theta}}^T} \boldsymbol{\Gamma}_\theta (\boldsymbol{\tau}_i - \sigma \hat{\boldsymbol{\theta}}) - \frac{\partial \alpha_{i-1}}{\partial \hat{\boldsymbol{\theta}}^T} \dot{\hat{\boldsymbol{\theta}}} \right) - \tilde{\boldsymbol{\nu}}_i^T \mathbf{P}_i^{-1} \dot{\tilde{\boldsymbol{\nu}}}_i$$

$$\dot{V}_i \leq - \sum_{j=1}^i (k_j - \frac{1}{2}) z_j^2 + z_i z_{i+1} - \sum_{j=1}^i \frac{b_j}{2} \tilde{\boldsymbol{\nu}}_j^T \tilde{\boldsymbol{\nu}}_j + \tilde{\boldsymbol{\theta}}^T (\boldsymbol{\tau}_i - \boldsymbol{\Gamma}_\theta^{-1} \dot{\hat{\boldsymbol{\theta}}}) - \sum_{j=2}^i z_j \frac{\partial \alpha_{j-1}}{\partial \hat{\boldsymbol{\theta}}^T} \boldsymbol{\Gamma}_\theta (\boldsymbol{\tau}_i - \sigma \hat{\boldsymbol{\theta}} - \boldsymbol{\Gamma}_\theta^{-1} \dot{\hat{\boldsymbol{\theta}}}) + \eta_i \quad (36)$$

where $\eta_i = \sum_{j=1}^i (\frac{b_j}{2} \boldsymbol{\nu}_j^{*T} \boldsymbol{\nu}_j^* + \frac{1}{2} \iota_j^2)$

Step n: Furthermore, to alleviate the communication burden, the following relative threshold event-triggered control is introduced

$$\begin{cases} \omega(t) = v(t_k) \quad \forall t \in [t_k, t_{k+1}) \\ t_{k+1} = \{t \in \Re \mid e(t) \geq \varpi |\omega(t)| + m_1\} \end{cases} \quad (37)$$

where $e(t) = v(t) - \omega(t)$ represents the measurement error and ϖ , m_1 are design parameters with $0 < \varpi < 1$, $m_1 > 0$. If the inequality in (36) holds, the moment is updated as t_{k+1} and the actual control signal is equal to $\omega(t_{k+1})$. Otherwise, the desired control signal $v(t)$ maintains the input control signal $\omega(t_k)$ with $t \in [t_k, t_{k+1})$.

Invoking (13), the state space equation of the considered system can be rewritten as:

$$\begin{cases} \dot{x}_i = x_{i+1} + \boldsymbol{\theta}^T \phi_i(\bar{\mathbf{x}}_i) + \Delta_i(\bar{\mathbf{x}}_i, t) & i = 1, 2 \cdots n-1 \\ \dot{x}_n = u_d(t) + \tilde{\boldsymbol{\theta}}^T \mathbf{F} + \varepsilon(t) + \boldsymbol{\theta}^T \phi_n(\mathbf{x}) + \Delta_n(\mathbf{x}, t) \\ y = x_1 \end{cases} \quad (38)$$

By (17) and (38), the derivative of z_n can be given as

$$\begin{aligned} \dot{z}_n = & u_d(t) + \tilde{\boldsymbol{\theta}}^T \mathbf{F} + \varepsilon(t) + \boldsymbol{\theta}^T \phi_n(\mathbf{x}) + \Delta_n(\mathbf{x}, t) - x_{1d}^{(n)} - \sum_{j=1}^{n-1} \frac{\partial \alpha_{n-1}}{\partial x_j} (x_{j+1} + \boldsymbol{\theta}^T \phi_j(\bar{\mathbf{x}}_j) + \Delta_j(\bar{\mathbf{x}}_j, t)) \\ & - \sum_{j=1}^{n-1} \frac{\partial \alpha_{n-1}}{\partial x_{1d}^{(j)}} x_{1d}^{(j)} - \sum_{j=1}^{n-1} \frac{\partial \alpha_{j-1}}{\partial \boldsymbol{\nu}_j^T} \dot{\boldsymbol{\nu}}_j - \frac{\partial \alpha_{n-1}}{\partial \hat{\boldsymbol{\theta}}^T} \dot{\hat{\boldsymbol{\theta}}} \end{aligned} \quad (39)$$

An RBFNN $\boldsymbol{\nu}_n^{*T} \zeta_n(\mathbf{x}) + \delta_n$ is used to approximate $\Delta_i(\mathbf{x}, t) - \sum_{j=1}^{i-1} \frac{\partial \alpha_{n-1}}{\partial x_j} \Delta_j(\bar{\mathbf{x}}_j, t)$, that is

$$\Delta_i(\mathbf{x}, t) - \sum_{j=1}^{i-1} \frac{\partial \alpha_{i-1}}{\partial x_j} \Delta_j(\bar{\mathbf{x}}_j, t) = \boldsymbol{\nu}_n^{*T} \zeta_n(\mathbf{x}) + \delta_n \quad (40)$$

Now, the desired control signal $u_d(t)$, the tuning function τ_n , the adaptive law $\dot{\hat{\boldsymbol{\theta}}}$ for unknown system parameters, the adaptive law $\dot{\hat{\boldsymbol{\nu}}}$ for unknown hysteresis parameters and the adaptive law $\dot{\boldsymbol{\nu}}_n$ for weights of RBFNN are constructed as

$$\left\{ \begin{aligned} u_d(t) = & -k_n z_n - z_{n-1} + x_{1d}^{(n)} + \sum_{j=1}^{n-1} \frac{\partial \alpha_{n-1}}{\partial x_j} x_{j+1} - \boldsymbol{\nu}_n^T \zeta_n(\mathbf{x}) - \hat{\boldsymbol{\theta}}^T (\phi_n(\mathbf{x}) - \sum_{j=1}^{n-1} \frac{\partial \alpha_{n-1}}{\partial x_j} \phi_j(\bar{\mathbf{x}}_j)) \\ & + \sum_{j=1}^{n-1} \frac{\partial \alpha_{n-1}}{\partial x_{1d}^{(j)}} x_{1d}^{(j)} + \sum_{j=1}^{n-1} \frac{\partial \alpha_{j-1}}{\partial \boldsymbol{\nu}_j^T} \dot{\boldsymbol{\nu}}_j + \frac{\partial \alpha_{n-1}}{\partial \hat{\boldsymbol{\theta}}^T} \Gamma_\theta (\tau_n - \sigma \hat{\boldsymbol{\theta}}) \\ \tau_n = & \tau_{n-1} + (\phi_n(\mathbf{x}) - \sum_{j=1}^{n-1} \frac{\partial \alpha_{n-1}}{\partial x_j} \phi_j(\bar{\mathbf{x}}_j)) z_n \\ \dot{\hat{\boldsymbol{\theta}}} = & \Gamma_\theta \tau_n - \Gamma_\theta \sigma \hat{\boldsymbol{\theta}} \\ \dot{\hat{\boldsymbol{\nu}}} = & \Gamma_\nu \mathbf{F} z_n - \Gamma_\nu \varsigma \hat{\boldsymbol{\nu}} \\ \dot{\boldsymbol{\nu}}_n = & \mathbf{P}_n \zeta_n(\mathbf{x}) z_n - b_n \mathbf{P}_n \boldsymbol{\nu}_n \end{aligned} \right. \quad (41)$$

where $k_n > 0$, $\sigma > 0$, $\varsigma > 0$ and $b_n > 0$ are positive constants, Γ_θ , Γ_ν and \mathbf{P}_n are all positive definite matrices.

Remark 7. It is notable that the desired control signal $u_d(t)$ will experience the estimated inverse hysteresis model(10), the event-triggered mechanism (37), and the hysteresis model successively to generate the actual control signal $u(t)$.

Substituting (40) and (41) into (39), one has

$$\dot{z}_n \leq -k_n z_n - z_{n-1} + \tilde{\boldsymbol{\nu}}_n^T \zeta_n(\mathbf{x}) + \tilde{\boldsymbol{\theta}}^T \mathbf{F} + \varepsilon(t) + \delta_n + \tilde{\boldsymbol{\theta}}^T (\phi_n(\mathbf{x}) - \sum_{j=1}^{n-1} \frac{\partial \alpha_{n-1}}{\partial x_j} \phi_j(\bar{\mathbf{x}}_j)) + \frac{\partial \alpha_{n-1}}{\partial \hat{\boldsymbol{\theta}}^T} \Gamma_\theta (\tau_n - \sigma \hat{\boldsymbol{\theta}} - \Gamma_\theta^{-1} \dot{\hat{\boldsymbol{\theta}}}) \quad (42)$$

Consider the following Lyapunov function V_n as

$$V_n = V_{n-1} + \frac{1}{2} z_n^2 + \frac{1}{2} \tilde{\boldsymbol{\nu}}_n^T \mathbf{P}_n^{-1} \tilde{\boldsymbol{\nu}}_n + \frac{1}{2} \tilde{\boldsymbol{\theta}}^T \Gamma_\theta^{-1} \tilde{\boldsymbol{\theta}} \quad (43)$$

By (42), the derivative of V_n is given by

$$\begin{aligned} \dot{V}_n &= \dot{V}_{n-1} + z_n \dot{z}_n - \tilde{\nu}_n^T \mathbf{P}_n^{-1} \dot{\nu}_n - \tilde{\theta}^T \Gamma_\theta^{-1} \dot{\hat{\theta}} \\ &\leq - \sum_{j=1}^{n-1} (k_j - \frac{1}{2}) z_j^2 - k_n z_n^2 - \sum_{j=1}^{n-1} \frac{b_j}{2} \tilde{\nu}_j^T \tilde{\nu}_j + \eta_{n-1} - \sum_{j=2}^n z_j \frac{\partial \alpha_{j-1}}{\partial \hat{\theta}^T} \Gamma_\theta (\tau_{n-1} - \sigma \hat{\theta} - \Gamma_\theta^{-1} \dot{\hat{\theta}}) \\ &\quad + \tilde{\theta}^T (\tau_n - \Gamma_\theta^{-1} \dot{\hat{\theta}}) + \tilde{\nu}_n^T \mathbf{P}_n^{-1} (\mathbf{P}_n \zeta_n(\mathbf{x}) z_n - \dot{\nu}_n) + \tilde{\theta}^T \Gamma_\theta^{-1} (\Gamma_\theta \mathbf{F} z_n - \dot{\hat{\theta}}) + z_n \epsilon(t) + \delta_n z_n \end{aligned} \quad (44)$$

Invoking (14)-(16), (35) and the three adaptive laws $\dot{\hat{\theta}}$, $\dot{\hat{\vartheta}}$, and $\dot{\nu}_n$ in (41), one has

$$\dot{V}_n \leq - \sum_{j=1}^{n-1} (k_j - \frac{1}{2}) z_j^2 - (k_n - 1) z_n^2 - \frac{\sigma}{2} \tilde{\theta}^T \tilde{\theta} - \sum_{j=1}^n \frac{b_j}{2} \tilde{\nu}_j^T \tilde{\nu}_j - \frac{\varsigma}{2} \tilde{\vartheta}^T \tilde{\vartheta} + \frac{\sigma}{2} \hat{\theta}^T \hat{\theta} + \frac{b_n}{2} \nu_n^T \nu_n + \frac{\varsigma}{2} \hat{\vartheta}^T \hat{\vartheta} + \frac{1}{2} \epsilon^2 + \frac{1}{2} l_n^2 + \eta_n \quad (45)$$

where $\eta_n = \sum_{j=1}^n (\frac{b_j}{2} \nu_j^{*T} \nu_j^* + \frac{1}{2} l_j^2)$

3.2 | System Stability Analysis

Theorem 1. For nonlinear system (1) under Assumptions 1,3 and ??, the control scheme developed in (26), (32), (41), it can be guaranteed that the nonlinear system suffered with parametric uncertainties, the uncertain nonlinear functions and the unknown hysteresis nonlinearity is ultimately bounded and the communication cost is reduced effectively. All the system signals are bounded and the tracking error, the estimation errors all converge to a bounded compact set.

Proof of Theorem 1. Denote the following equations

$$\Xi = \frac{\sigma}{2} \hat{\theta}^T \hat{\theta} + \frac{b_n}{2} \nu_n^T \nu_n + \frac{\varsigma}{2} \hat{\vartheta}^T \hat{\vartheta} + \frac{1}{2} \epsilon^2 + \frac{1}{2} l_n^2 + \eta_{n-1} \quad (46)$$

$$\kappa = \min \left\{ 2k_1 - 1, \dots, 2k_n - 2, \dots, \frac{\sigma}{\lambda_{\max}(\Gamma_\theta^{-1})}, \frac{b_1}{\lambda_{\max}(\mathbf{P}_1^{-1})}, \dots, \frac{b_n}{\lambda_{\max}(\mathbf{P}_n^{-1})}, \frac{\varsigma}{\lambda_{\max}(\Gamma_\vartheta^{-1})} \right\} \quad (47)$$

where $\lambda_{\max}(\cdot)$ represents maximum eigenvalue of a matrix.

From (45)-(47), it could be obtained that

$$\dot{V}_n \leq -\kappa V_n + \Xi \quad (48)$$

Integrating inequality (48), we have

$$V_n \leq e^{-\kappa t} V_n(0) + \frac{\Xi}{\kappa} \quad (49)$$

Then,

$$\lim_{t \rightarrow \infty} V_n(t) \leq \frac{\Xi}{\kappa} \quad (50)$$

which implies $\lim_{t \rightarrow \infty} \|z\| \leq \sqrt{\frac{2\Xi}{\kappa}}$ with $z = [z_1, \dots, z_n]^T$. The estimation error of parametric uncertainties $\tilde{\theta}$, the estimation error of unknown hysteresis parameter $\tilde{\vartheta}$ and the estimation error of RBFNN weights $\tilde{\nu}_i$ can also have the upper bound. That means the boundedness of z , $\tilde{\theta}$, $\tilde{\vartheta}$ and $\tilde{\nu}_i$ is ensured. From the control signal α_i in (20), (26), (32) is also bounded for $i = 1, \dots, n-1$. The boundedness of the desired control signal $\omega(t)$ can also be deduced based on (41), (37) and (10). From (17) and Assumption 1, it is concluded that all the closed-loop system signals \mathbf{x} are bounded. Moreover, by observing the inequality in (50), the range of compact set depends on Ξ and κ related to the adjustable variables. \square

4 | SIMULATION RESULTS

To verify the effectiveness of the developed control algorithm, the second-order system described by the following expressions, is considered:

$$\begin{aligned}\dot{x}_1 &= x_2 + \boldsymbol{\theta}^T \phi_1(x_1) + \Delta_1(x_1, t) \\ \dot{x}_2 &= H[v](t) + \boldsymbol{\theta}^T \phi_2(\mathbf{x}) + \Delta_2(\mathbf{x}, t) \\ y &= x_1\end{aligned}\quad (51)$$

where $\phi_1(x_1) = x_1$ and $\phi_2(\bar{\mathbf{x}}_2) = x_2 + x_1$ are known for control design. x_1, x_2 denote the system states and $\mathbf{x} = [x_1, x_2]^T$, while y is the output signal. $\Delta_1(x_1, t) = \sin(x_1)$, $\Delta_2(\mathbf{x}, t) = \sin(x_1 x_2)$. $H[v](t)$ denotes the unknown hysteresis effect and v is the intermediate control signal. In the simulation, the discrete model is employed to depict the hysteresis phenomenon.

$$u(t) = H[v](t) = p_{0s}v(t) - \sum_{i=1}^m p_i(r_i)F_{r_i}[v](t)\Delta r_i \quad (52)$$

where $p_{0s} = 3.2$, $m = 100$, $r_i = 0.1i$, $p_i(r_i) = 0.8e^{-0.002(r_i)^2}$ and $\Delta r_i = 1$ for $i = 1, \dots, m$. The curve of the hysteresis is depicted in Fig. 2, where the input signal is chosen as $v = \sin 2t$.

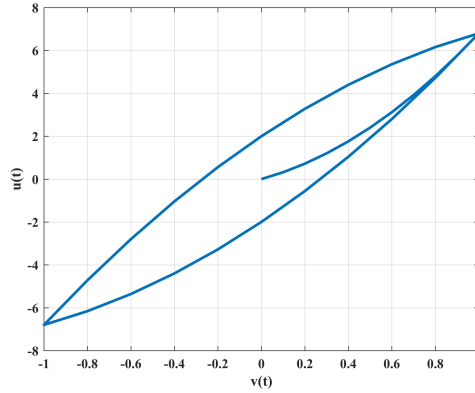


FIGURE 2 Tracking errors of the comparative controllers.

To illustrate the effectiveness of the developed controller, the following two controllers need to be compared. In simulated software, the sampling interval time is 0.001s.

1) HIETC-ANNRC: This is the proposed event-triggered adaptive estimated inverse neural network controller, described in Section III. To fulfill the control goal, the adjustable coefficients are obtained via trial-and-error method. The gain coefficients are chosen as $k_1 = 20$, $k_2 = 10$, the parameter adaptation gains of parametric uncertainties are set as $\boldsymbol{\Gamma}_\theta = \text{diag}\{10, 20\}$, $\sigma = 1 \times 10^{-2}$. It should be mentioned that we find that it is not necessary to set the number of discrete intervals of hysteresis inverse (10) as the same as it in hysteresis model (52). The distinct effect can be obtained by the hysteresis inverse mechanism when the number m is chosen as 2. In other words, there are three unknown parameters of hysteresis inverse model needing estimating by the adaptive law, then $\hat{\boldsymbol{\theta}} = [\hat{p}_{0s}, -\hat{\theta}_1, -\hat{\theta}_2]^T$, $\mathbf{F} = [v(t), F_{r_1}[v](t), F_{r_2}[v](t)]^T$, the parameter adaptation gains are set as $\boldsymbol{\Gamma}_\theta = \text{diag}\{50, 50, 100\}$ and $\varsigma = 1 \times 10^{-2}$. The parameters in the event-triggered mechanism is set as $\varpi = 0.1$ and $m_1 = 0.01$. There are two RBFNN in the simulation, the nodes of the first one is 3, the weight adaption rate is chosen as $\mathbf{P}_1 = \text{diag}\{5, 5, 5\}$ and $b_1 = 1 \times 10^{-4}$. The nodes of the other is 5 and the weight adaption rate is set as $\mathbf{P}_2 = \text{diag}\{10, 10, 10, 10, 10\}$ and $b_2 = 10$. The width values of Gaussian functions are set as $d_1 = 3$ and $d_2 = 2$, respectively. Finally, the initial values are all zero. The specific expressions of

TABLE 1 Performance indices for the last 10 seconds.

<i>Indexes</i>	<i>ME</i>	<i>ATD</i>	<i>STD</i>
HIETC-ANNRC	0.0038	0.0013	0.0009
ANNRC	0.0127	0.0060	0.0026

the control scheme are given as follows:

$$\begin{cases} \alpha_1 = -k_1 z_1 - \hat{\theta}^T \phi_1(x_1) - \nu_1^T \zeta_1(x_1) \\ \tau_1 = \phi_1(x_1) z_1 \\ \dot{\nu}_1 = P_1 \zeta_1(x_1) z_1 - b_1 P_1 \nu_1 \end{cases} \quad (53)$$

$$\begin{cases} u_d(t) = -k_2 z_2 - z_1 + \frac{\partial \alpha_1}{\partial x_1} x_2 + x_{1d}^{(2)} \\ \quad - \nu_2^T \zeta_2(x) - \hat{\theta}^T (\phi_2(x) - \frac{\partial \alpha_1}{\partial x_1} \phi_1(x_1)) \\ \quad + \frac{\partial \alpha_1}{\partial x_{1d}} x_{1d}^{(1)} + \frac{\partial \alpha_1}{\partial \nu_1^T} \dot{\nu}_1 + \frac{\partial \alpha_1}{\partial \hat{\theta}^T} \Gamma \tau_1 \\ \tau_2 = \tau_1 + (\phi_2(x) - \frac{\partial \alpha_1}{\partial x_1} \phi_1(x_1)) z_2 \\ \dot{\hat{\theta}} = \Gamma_\theta \tau_2 - \Gamma_\theta \sigma \hat{\theta} \\ \dot{\hat{\vartheta}} = \Gamma_\vartheta F z_2 - \Gamma_\vartheta \varsigma \hat{\vartheta} \\ \dot{\nu}_2 = P_2 \zeta_2(x) z_2 - b_2 P_2 \nu_2 \end{cases} \quad (54)$$

2) ANNRC: Compared with the proposed HIETC-ANNRC, ANNRC lacks both event-triggered law and the estimated hysteresis inverse model. We just need to connect the desired control signal $u_d(t)$ directly to the plant without experiencing other loops, the controller of ANNRC can be realized.

To further assess the performances of above four controller in a quantified way, the following three performance indices, i.e., maximum *ME*, average *ATD*, and standard deviation *STD* of tracking error are employed whose expressions have been defined in⁴¹.

To illustrate the superiority of the developed controller, the following four controllers are tested for a smooth enough sinusoidal-like reference trajectory $x_{1d}(t) = \sin(t)(1 - e^{-0.5t})$. The simulation results are shown in Fig. 3-Fig. 8. The tracking performances of them are presented in Fig. 3. The trajectory output of the proposed controller HIETC-ARNNC is almost identical with the desired motion signal. It is more apparent to analyze the performance of the two controllers based on the tracking errors of them depicted in Fig. 4 and the performance indices for the last 10 seconds of them given in Table 1. The HIETC-ARNNC and ARNNC controllers lead to the *STD* errors of 0.0009 and 0.0026, respectively. The tracking accuracy of HIETC-ARNNC has been improved by 65.3% over ARNNC scheme. From these analysis, it can be evidently found that the proposed HIETC-ANNRC exhibits an excellent performance where the hysteresis nonlinearity has been suppressed to a negligible level by the hysteresis inverse compensation scheme. The estimations of the unknown hysteresis parameters and the system parametric uncertainties are presented in Fig. 5 and Fig. 6, and both of them exhibit the convergent trend.

Finally, the controller signal after ETC is utilized to control the plant, which can reduce the communication resource and calculation resource. Fig. 7 reveals that the ETC generates the control signal $\omega(t)$, which is only updated when the condition of event-trigger holds. The time interval of event triggered is depicted in Fig. 8. Different from the traditional time-triggered control scheme, the time interval is not equal to the sampling time 0.001s. The maximum of the time interval is 1.062s, which means the control signal remains unchanged during this period. Comparing with the number of sampling 40000, the number of event triggered is 555 during the whole control period 40s.

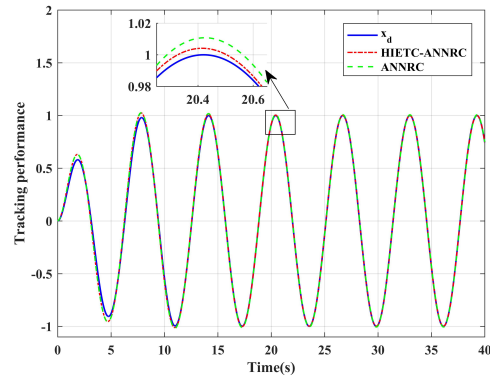


FIGURE 3 Tracking performances of the four comparative controllers.

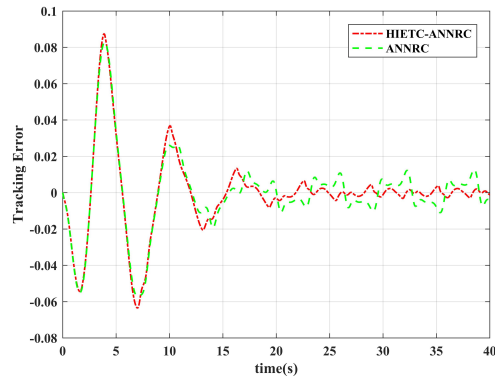


FIGURE 4 Tracking errors of the comparative controllers.

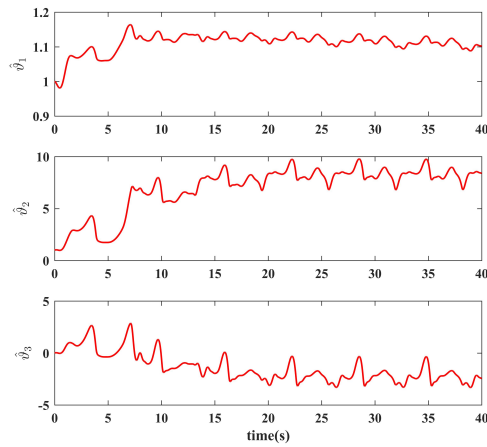


FIGURE 5 Hysteresis parameter estimations $\hat{\vartheta}_1, \hat{\vartheta}_2, \hat{\vartheta}_3$.

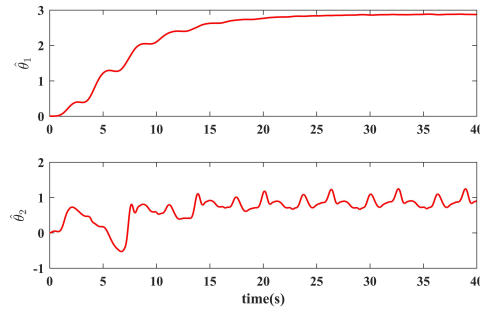


FIGURE 6 System parameter estimations $\hat{\theta}_1, \hat{\theta}_2$.

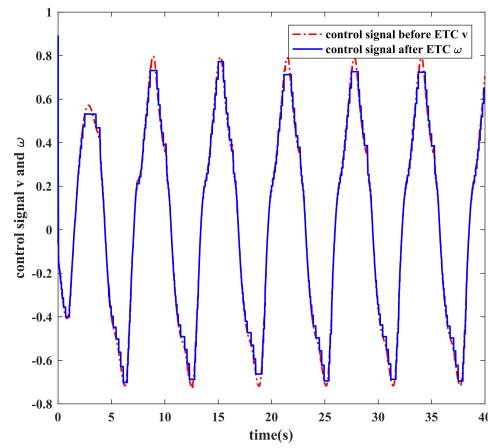


FIGURE 7 Control signal before and after the ETC.

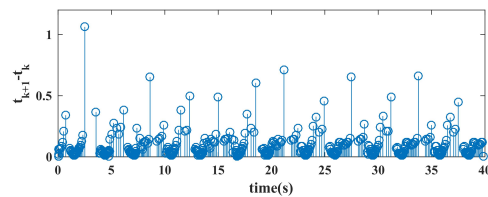


FIGURE 8 Time interval of event triggered.

5 | CONCLUSION

This paper develops an event-triggered adaptive estimated inverse controller for a class of uncertain nonlinear system subjected to parametric uncertainties, unknown nonlinear functions and the Prandtl–Ishlinskii (PI) hysteresis input, simultaneously. The radial basis functions neural network is applied to compensate the uncertain nonlinear functions whose weights are obtained by the adaptive technique. Moreover, the parametric uncertainties are also suppressed through the adaptive law. The distinct novelty of this paper lies in that the adaptive estimated hysteresis inverse model is developed, which is utilized to make up for the unknown hysteresis effect online. Furthermore, an event-triggered adaptive estimated inverse neural network control strategy

is proposed through the backstepping technique. Finally, the results of the numerical simulation verify the superiority of the developed controller with the communication resource saved.

AUTHOR CONTRIBUTIONS

Ning Zhou: Conceptualization, Methodology, Writing – original draft, Software, Validation. Jianyong Yao: Supervision. Wenxiang Deng: Writing - review & editing.

ACKNOWLEDGMENTS

This work was supported in part by the National Key R&D Program of China under Grant 2021YFB2011300, in part by the National Natural Science Foundation of China under Grant 52275062, in part by the Postgraduate Research & Practice Innovation Program of Jiangsu Province under Grant KYCX23_0421.

CONFLICT OF INTEREST

The authors have no conflicts of interest to declare.

REFERENCES

1. Rakotondrabe M. Bouc–Wen modeling and inverse multiplicative structure to compensate hysteresis nonlinearity in piezoelectric actuators. *IEEE Transactions on Automation Science and Engineering*. 2010;8(2):428–431.
2. Gu GY, Yang MJ, Zhu LM. Real-time inverse hysteresis compensation of piezoelectric actuators with a modified Prandtl-Ishlinskii model. *Review of Scientific Instruments*. 2012;83(6):065106.
3. Hucko S, Matthiesen G, Reinertz O, Schmitz K. Investigation of Magnetic Force Hysteresis in Electromechanical Actuators. *Chemical Engineering & Technology*. 2023;46(1):158–166.
4. Hucko S, Krampe H, Schmitz K. Evaluation of a Soft Sensor Concept for Indirect Flow Rate Estimation in Solenoid-Operated Spool Valves. In: . 12. MDPI. 2023:148.
5. Tao G, Kokotovic PV. Adaptive control of plants with unknown hystereses. *IEEE Transactions on Automatic Control*. 1995;40(2):200–212.
6. Su CY, Wang Q, Chen X, Rakheja S. Adaptive variable structure control of a class of nonlinear systems with unknown Prandtl-Ishlinskii hysteresis. *IEEE Transactions on automatic control*. 2005;50(12):2069–2074.
7. Wang Q, Su CY. Robust adaptive control of a class of nonlinear systems including actuator hysteresis with Prandtl–Ishlinskii presentations. *Automatica*. 2006;42(5):859–867.
8. Yao B, Bu F, Reedy J, Chiu GC. Adaptive robust motion control of single-rod hydraulic actuators: theory and experiments. *IEEE/ASME transactions on mechatronics*. 2000;5(1):79–91.
9. Sun W, Gao H, Kaynak O. Adaptive backstepping control for active suspension systems with hard constraints. *IEEE/ASME transactions on mechatronics*. 2012;18(3):1072–1079.
10. Xu L, Yao B. Adaptive robust precision motion control of linear motors with negligible electrical dynamics: theory and experiments. *IEEE/ASME transactions on mechatronics*. 2001;6(4):444–452.
11. Zhou S, Shen C, Xia Y, Chen Z, Zhu S. Adaptive robust control design for underwater multi-dof hydraulic manipulator. *Ocean Engineering*. 2022;248:110822.
12. Huang YJ, Kuo TC, Chang SH. Adaptive sliding-mode control for nonlinear systems with uncertain parameters. *IEEE Transactions on Systems, Man, and Cybernetics, Part B (Cybernetics)*. 2008;38(2):534–539.
13. Sakthivel R, Abinandhitha R, Harshavarthini S, Mohammadzadeh A, Saat S. Anti-disturbance observer-based finite-time reliable control design for fuzzy switched systems. *Fuzzy Sets and Systems*. 2023:108673.
14. Yang J, Li S, Yu X. Sliding-mode control for systems with mismatched uncertainties via a disturbance observer. *IEEE Transactions on industrial electronics*. 2012;60(1):160–169.
15. Xie WF. Sliding-mode-observer-based adaptive control for servo actuator with friction. *IEEE Transactions on Industrial Electronics*. 2007;54(3):1517–1527.
16. Yao J, Deng W. Active disturbance rejection adaptive control of uncertain nonlinear systems: Theory and application. *Nonlinear Dynamics*. 2017;89:1611–1624.
17. Li Y, Tong S, Li T. Adaptive fuzzy output feedback control of uncertain nonlinear systems with unknown backlash-like hysteresis. *Information Sciences*. 2012;198:130–146.
18. Yang X, Deng W, Yao J. Neural network based output feedback control for DC motors with asymptotic stability. *Mechanical Systems and Signal Processing*. 2022;164:108288.
19. Mayergoyz I. Mathematical models of hysteresis. *IEEE Transactions on magnetics*. 1986;22(5):603–608.
20. Kuhnen K. Modeling, identification and compensation of complex hysteretic nonlinearities: A modified Prandtl-Ishlinskii approach. *European journal of control*. 2003;9(4):407–418.
21. Ismail M, Ikhouane F, Rodellar J. The hysteresis Bouc-Wen model, a survey. *Archives of computational methods in engineering*. 2009;16:161–188.
22. Zhou J, Wen C, Zhang Y. Adaptive backstepping control of a class of uncertain nonlinear systems with unknown backlash-like hysteresis. *IEEE transactions on Automatic Control*. 2004;49(10):1751–1759.
23. Wang J, Liu Z, Zhang Y, Chen CP. Neural adaptive event-triggered control for nonlinear uncertain stochastic systems with unknown hysteresis. *IEEE Transactions on Neural Networks and Learning Systems*. 2019;30(11):3300–3312.
24. Lu K, Liu Z, Chen CP, Zhang Y. Event-triggered neural control of nonlinear systems with rate-dependent hysteresis input based on a new filter. *IEEE transactions on neural networks and learning systems*. 2019;31(4):1270–1284.
25. Chen X, Su CY, Fukuda T. Adaptive control for the systems preceded by hysteresis. *IEEE Transactions on Automatic Control*. 2008;53(4):1019–1025.

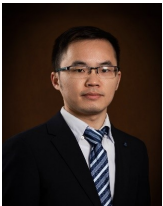
26. Feng Y, Hu YM, Su CY. Robust adaptive control for a class of perturbed strict-feedback nonlinear systems with unknown Prandtl-Ishlinskii hysteresis. In: IEEE. 2006:106–111.
27. Ren B, Ge SS, Su CY, Lee TH. Adaptive neural control for a class of uncertain nonlinear systems in pure-feedback form with hysteresis input. *IEEE Transactions on Systems, Man, and Cybernetics, Part B (Cybernetics)*. 2008;39(2):431–443.
28. Krejci P, Kuhnen K. Inverse control of systems with hysteresis and creep. *IEE Proceedings-Control Theory and Applications*. 2001;148(3):185–192.
29. Al Janaideh M, Krejčí P. Inverse rate-dependent Prandtl–Ishlinskii model for feedforward compensation of hysteresis in a piezomicropositioning actuator. *IEEE/ASME Transactions on mechatronics*. 2012;18(5):1498–1507.
30. Zhang X, Wang Y, Wang C, Su CY, Li Z, Chen X. Adaptive estimated inverse output-feedback quantized control for piezoelectric positioning stage. *IEEE transactions on cybernetics*. 2018;49(6):2106–2118.
31. Zhang X, Wang Y, Chen X, et al. Decentralized adaptive neural approximated inverse control for a class of large-scale nonlinear hysteretic systems with time delays. *IEEE Transactions on Systems, Man, and Cybernetics: Systems*. 2018;49(12):2424–2437.
32. Li Z, Hu Y, Liu Y, Chen T, Yuan P. Adaptive inverse control of non-linear systems with unknown complex hysteretic non-linearities. *IET control theory & applications*. 2012;6(1):1–7.
33. Liu S, Su CY, Li Z. Robust adaptive inverse control of a class of nonlinear systems with Prandtl-Ishlinskii hysteresis model. *IEEE Transactions on Automatic Control*. 2014;59(8):2170–2175.
34. Zhang X, Li Z, Su CY, Lin Y, Fu Y. Implementable adaptive inverse control of hysteretic systems via output feedback with application to piezoelectric positioning stages. *IEEE Transactions on industrial electronics*. 2016;63(9):5733–5743.
35. Su X, Liu Z, Zhang Y, Chen CP. Event-triggered adaptive fuzzy tracking control for uncertain nonlinear systems preceded by unknown Prandtl–Ishlinskii hysteresis. *IEEE Transactions on Cybernetics*. 2019;51(6):2979–2992.
36. Zhou Q, Wang W, Ma H, Li H. Event-triggered fuzzy adaptive containment control for nonlinear multiagent systems with unknown Bouc–Wen hysteresis input. *IEEE Transactions on Fuzzy Systems*. 2019;29(4):731–741.
37. Yang T, Zhang X, Fang Y, Sun N, Iwasaki M. Observer-Based Adaptive Fuzzy Event-Triggered Control for Mechatronic Systems With Inaccurate Signal Transmission and Motion Constraints. *IEEE/ASME Transactions on Mechatronics*. 2022;27(6):5208–5221.
38. Wang J, Zhang H, Ma K, Liu Z, Chen CP. Neural adaptive self-triggered control for uncertain nonlinear systems with input hysteresis. *IEEE transactions on neural networks and learning systems*. 2021;33(11):6206–6214.
39. Li Y, Liu Y, Tong S. Observer-based neuro-adaptive optimized control of strict-feedback nonlinear systems with state constraints. *IEEE Transactions on Neural Networks and Learning Systems*. 2021;33(7):3131–3145.
40. Xing X, Liu J. Event-triggered neural network control for a class of uncertain nonlinear systems with input quantization. *Neurocomputing*. 2021;440:240–250.
41. Yao J, Jiao Z, Ma D. Extended-state-observer-based output feedback nonlinear robust control of hydraulic systems with backstepping. *IEEE Transactions on Industrial electronics*. 2014;61(11):6285–6293.

AUTHOR BIOGRAPHY

Ning Zhou. received the B. Tech degree from the Yangzhou University, Yangzhou, China, in 2020. She is currently working towards the Ph.D degree in the School of Mechanical Engineering, Nanjing University of Science and Technology, Nanjing, 210094, China. Her current research interests include servo control of mechatronic systems and intelligent control of electro-hydraulic proportional servo valve.



Jianyong Yao. received the B. Tech degree from the Tianjin University, Tianjin, China, in 2006, and the Ph.D. degree in Mechatronics from the Beihang University, Beijing, China, in 2012. He was a visiting exchange student with the School of Mechanical Engineering, Purdue University, from Oct. 2010 to Oct. 2011. In 2012, he joined the School of Mechanical Engineering, Nanjing University of Science and Technology, Nanjing, China, and currently as a full professor. His current research interests include servo control of mechatronic systems, adaptive and robust control, fault detection and accommodation of dynamic systems.



Wenxiang Deng. received the B. Tech. degree in mechanical engineering from Central South University, Changsha, China, in 2013, and the Ph.D. degree in mechanical engineering from the Nanjing University of Science and Technology, Nanjing, China, in 2018. He is currently an Associate Professor with the School of Mechanical Engineering, Nanjing University of Science and Technology. His current research interests include servo control of mechatronic systems, hydraulic robot control, robust adaptive control, and nonlinear compensation.